

Aquation and Anation Kinetics of Rhenium(I) Dicarbonyl Complexes: Relation to Cell Toxicity and Bioavailability

Marietjie Schutte-Smith, Sierra C. Marker, Justin J. Wilson, and Hendrik G. Visser*

Cite This: *Inorg. Chem.* 2020, 59, 15888–15897

Read Online

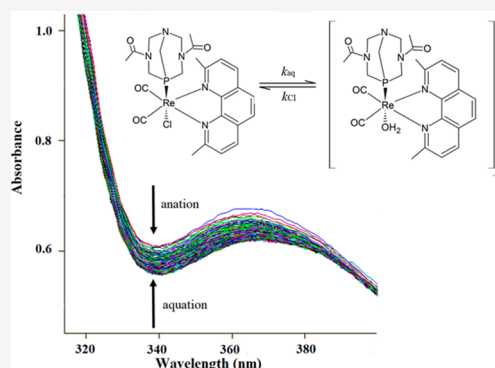
ACCESS |

Metrics & More

Article Recommendations

Supporting Information

ABSTRACT: The aquation reactions of four rhenium(I) dicarbonyl complexes, $[\text{Re}(\text{CO})_2(\text{NN})(\text{PR}_3)(\text{Cl})]$, where NN = 1,10-phenanthroline (Phen) and 2,9-dimethyl-1,10-phenanthroline (DMPhen) and PR_3 = 1,3,5-triaza-7-phosphaadamantane (PTA) and 1,4-diacetyl-1,3,7-triaza-5-phosphabicyclo[3.3.1]nonane (DAPTA). Additionally, the anation reactions of the corresponding aqua complexes with Cl^- were investigated. Single crystals of $[\text{Re}(\text{CO})_2(\text{DMPhen})(\text{PTA})(\text{Cl})]\cdot\text{DMF}$ and $[\text{Re}(\text{CO})_2(\text{DMPhen})(\text{DAPTA})(\text{Cl})]$ were obtained, and their structures were determined using X-ray diffraction. The Re–Cl interatomic distances are 2.4991(13) and 2.4922(6) Å, respectively, indicating a mild trans influence effect of the phosphine ligands. The rate constants, k_{aq} , for the aquation reactions of these complexes spanned a range of $(3.7 \pm 0.3) \times 10^{-4}$ to $(15.7 \pm 0.3) \times 10^{-4} \text{ s}^{-1}$ with the two Phen complexes having rate constants that are 2.5 times greater than those of the DMPhen complexes at 298 K. Similarly, the second-order anation rate constants (k_{Cl}) of the resulting aqua complexes, $[\text{Re}(\text{CO})_2(\text{NN})(\text{PR}_3)(\text{H}_2\text{O})]^+$, with Cl^- ions at 298 K varied between $(2.99 \pm 0.05) \times 10^{-3}$ and $(6.79 \pm 0.09) \times 10^{-3} \text{ M}^{-1} \text{ s}^{-1}$. Likewise, these rate constants for the Phen complexes were almost 2 times faster than those of the DMPhen complexes. The pK_a values of the four aqua complexes were determined to be greater than 9.0 for all of the complexes with $[\text{Re}(\text{CO})_2(\text{Phen})(\text{PTA})(\text{H}_2\text{O})]^+$ having the highest pK_a value of 9.28 ± 0.03 . From the pK_a values and the ratios of the aquation and anation rate constants, which give thermodynamic Cl^- binding constants, the speciation of the rhenium(I) complexes in blood plasma, the cytoplasm, and the cell nucleus were estimated. The data suggest that the aqua complexes would be the dominant species in all three environments. This result may have important implications on the potential biological activity of these complexes.



INTRODUCTION

Despite significant advances in our understanding of cancer, it is still one of the leading causes of death worldwide.¹ Among the most commonly used chemotherapeutic agents are the platinum-based drugs, cisplatin, carboplatin, and oxaliplatin. Unfortunately, the potent anticancer activities of these complexes are accompanied by severe side effects, and cancer cells can readily develop resistance to them.^{2–6} Therefore, significant research efforts have been directed toward finding complexes of alternative metal ions that can overcome the limitations of conventional platinum-based drugs. In particular, the third-row transition metals neighboring platinum, namely, rhenium, osmium, and iridium, have chemical properties that are similar to this element, but offer more structural, photophysical, and redox diversity.^{7–10}

There has been significant interest in rhenium(I) tricarbonyl complexes for their use in radiopharmacy, photocatalysis, and, more recently, chemotherapy.^{11–25} To access a diverse range of drug candidates, the *fac*- $[\text{Re}(\text{CO})_3(\text{H}_2\text{O})_3]^+$ synthon enables a wide range of rhenium(I) tricarbonyl complexes to be obtained by displacing the three labile water ligands with alternative ligands.^{26–30} The rhenium(I) tricarbonyl core of the resulting molecules is highly stable *in vivo*, enabling the

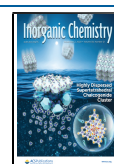
target specificity, lipophilicity, photophysical properties, and redox potentials to be tuned by the supporting ligands.³¹

Rhenium(I) dicarbonyl complexes have not had much attention for use as direct chemotherapeutic agents,^{32–34} although they are formed after CO release from mostly tricarbonyl complexes.^{14,35–37}

Although the mechanism of the anticancer activity of rhenium(I) carbonyl complexes is poorly understood, several studies have suggested that the biological activities of these complexes involve interactions with DNA through either intercalation, groove binding, or the direct formation of covalent adducts.^{18,38,39} A complicating factor in studying the mechanisms of action of these complexes, however, is the fact that they can undergo ligand substitution reactions in cells with biological nucleophiles, changing their structures and proper-

Received: August 12, 2020

Published: October 21, 2020



ties.^{40–43} Therefore, investigating the reactivity and stability of potential rhenium-based chemotherapeutic agents in a controlled chemical environment can provide important insight on the types and time scales of the transformations that these complexes undergo in biological media. In addition, the mechanism of ligand substitution may also have significant implications on the biological stabilities of these complexes if a dissociative mechanism is operative for example; the uptake of the complex *in vivo* would be limited to structural changes in its immediate coordination sphere since the rate of substitution would be independent from nucleophilic attack of biosubstrates and *vice versa*. The ligand substitution reactions of Re(I) tricarbonyl complexes have been studied extensively,^{44–53} with the earliest studies looking at the complex formation reactions of *fac*-[Re(CO)₃(H₂O)₃]⁺ with various monodentate ligands such as pyrazine and dimethyl sulfide.⁵¹ It was concluded that a mechanistic changeover from interchange dissociative (*I_d*) to interchange associative (*I_a*) occurs when moving from harder ligands to the softer S-donor ligands. The substitution processes of *fac*-[Re(CO)₃(bid)(L)]ⁿ (bid = bidentate ligand; *n* = 0, +1) showed a strong dependence on the nature of the bidentate ligand. For example, it was demonstrated that the reaction rates can be tuned over a factor of 20,000 and that the intimate mechanism of substitution depends on the type of bidentate ligand employed.^{43,44,46,54} Recently, high-pressure kinetic studies from our laboratory indicated that the substitution of methanol from *fac*-[Re(Trop)(CO)₃(MeOH)] (Trop = tropolonato) follows an interchange dissociative (*I_d*) mechanism.⁴³

Despite these significant advances in understanding factors that affect ligand substitution processes of Re(I) tricarbonyl complexes, to date these studies have not been extended to Re(I) dicarbonyl complexes. It is important to understand the ligand substitution processes of these complexes because it was recently demonstrated that *fac*-[Re(CO)₃(NN)(PR₃)]⁺ (NN = diimine ligand; PR₃ = 1,3,5-triaza-7-phosphaadamantane (PTA), tris(hydroxymethyl)phosphine (THP), or 1,4-diacetyl-1,3,7-triaza-5-phosphabicyclo[3.3.1]nonane (DAPTA)) complexes undergo photostitution of a CO ligand upon exposure to 365 nm light and form a bioactive Re(I) dicarbonyl complex.⁵⁵ Of all of the complexes studied, *fac*-[Re(CO)₃(Phen)(DAPTA)]⁺ (Phen = 1,10 phenanthroline) was the most cytotoxic upon irradiation. The dicarbonyl photoproducts, [Re(CO)₂(NN)(PR₃)(L)]ⁿ (L = Cl⁻ or OH₂; *n* = 0, +1), were also separately synthesized and evaluated for cytotoxicity. Although the cytotoxic activity of the dicarbonyl complexes was low, the release of CO and singlet oxygen (¹O₂) also contributed to the large phototoxic response.

On the basis of the potential of Re(I) dicarbonyl complexes such as photoactive anticancer agents, we sought to understand the ligand substitution processes that could affect their biological activities, namely, aquation and anation. The importance of aquation reactions of metal-based anticancer agents in biological systems has been well documented.^{21,41–43,55–58} Furthermore, the acid dissociation constants and equilibrium constants of metal–aqua species are critical for determining their speciation under various biological conditions. For example, the chloride concentration in blood plasma is high (about 104 mM) and much lower in the cytoplasm (22.7 mM) and nucleus (4 mM). Therefore, on the basis of equilibrium considerations, aquation of metal–chlorido complexes is expected to be suppressed in blood plasma to a greater extent than that in the nucleus. On the

other hand, p*K_a* values of the resulting metal–aqua complexes provide information on the ratio of chemically inert hydroxo and labile aqua species at any given moment, whereas cisplatin exhibits p*K_a* values of 5.39 and 7.21, indicating that the dominant species in the cell are monohydroxo and dihydroxo species.⁵⁷

We report here the synthesis of a small library of Re(I) dicarbonyl complexes of the form [Re(CO)₂(NN)(PR₃)(L)]ⁿ, where NN = 1,10-phenanthroline (Phen) or 2,9-dimethyl 1,10-phenanthroline (DMPhen), PR₃ = PTA or DAPTA, and L = H₂O or Cl⁻ (Figure 1). The crystal structures of *fac*-

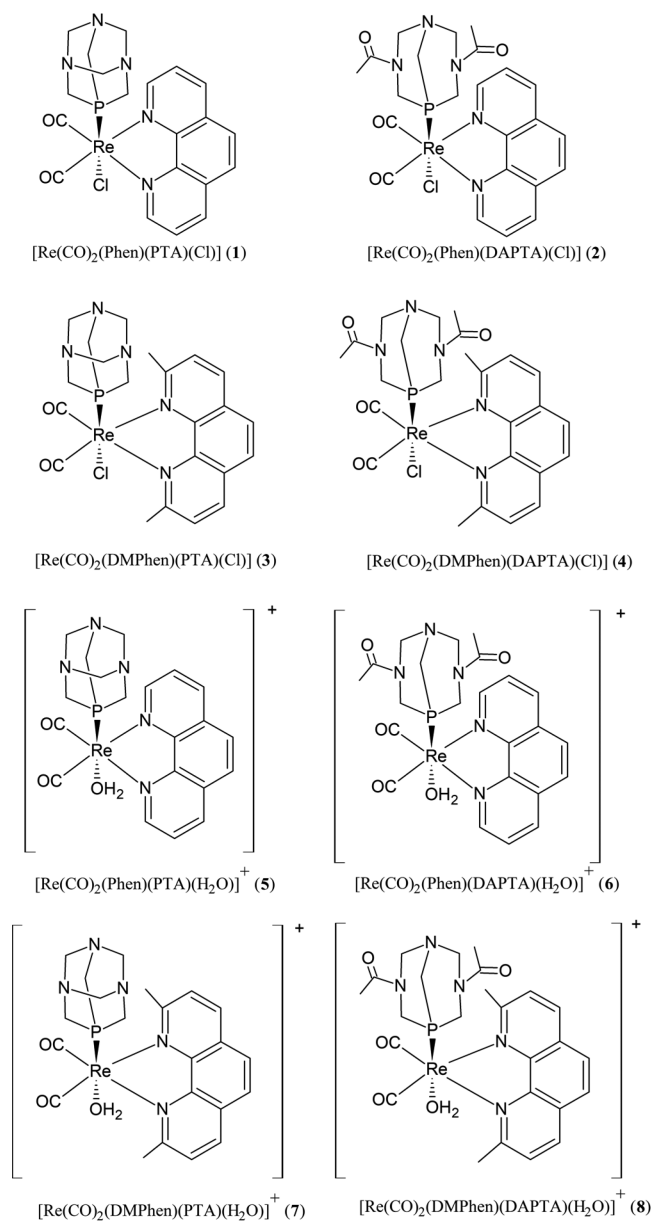


Figure 1. Illustration of the structures of rhenium complexes 1–8.

[Re(CO)₂(DMPhen)(DAPTA)(Cl)]·DMF (3a) and *fac*-[Re(CO)₂(Phen)(PTA)(Cl)] are also included. The aquation of [Re(CO)₂(Phen)(PTA)(Cl)] (1), [Re(CO)₂(Phen)(DAPTA)(Cl)] (2), [Re(CO)₂(DMPhen)(PTA)(Cl)] (3), and [Re(CO)₂(DMPhen)(DAPTA)(Cl)] (4) was investigated at pH = 5.0 at different ionic strengths. The substitution reactions of the aqua ligands of the complexes [Re-

(CO)₂(Phen)(PTA)(H₂O)]⁺ (5), [Re(CO)₂(Phen)-(DAPTA)(H₂O)]⁺ (6), [Re(CO)₂(DMPhen)(PTA)(H₂O)]⁺ (7), and [Re(CO)₂(DMPhen)(DAPTA)(H₂O)]⁺ (8) under different ionic strengths and at different temperatures were also explored. These studies allow for the determination of the activation parameters of the complexes, and they provide insight into the intimate mechanism of these reactions.

EXPERIMENTAL SECTION

Methods and Materials. Rhenium carbonyl was purchased from Pressure Chemicals (Pittsburgh, PA, USA). Re(CO)₅Cl was synthesized as previously reported.⁵⁵ The diimine ligands, Phen and DMPhen, were purchased from either Sigma-Aldrich (St. Louis, MO, USA) or Alfa Aesar (Heysham, England) and were used as received. [Re(CO)₃(Phen)Cl] and [Re(CO)₃(DMPhen)Cl] were synthesized using a previously reported procedure.^{59,60} The phosphine ligand, PTA, was purchased from Alfa Aesar and was used as received. DAPTA was synthesized from PTA using a previously reported procedure.⁶¹ The corresponding Re(I) tricarbonyl complexes, [Re(CO)₃(Phen)(PTA)]⁺, [Re(CO)₃(Phen)(DAPTA)]⁺, [Re(CO)₃(DMPhen)(PTA)]⁺, and [Re(CO)₃(DMPhen)(DAPTA)]⁺, were synthesized as previously described.⁵⁵ All solvents were ACS grade or higher. All reactions were carried out under ambient atmospheric conditions without any effort to exclude water or oxygen.

Physical Measurements. NMR samples were prepared as solutions using DMSO-*d*₆ and D₂O as the solvent. NMR spectra were acquired on a Varian Inova 400 MHz and a Bruker 400 MHz spectrometer. ¹H NMR chemical shifts were referenced to residual solvent peaks vs tetramethylsilane (TMS) at 0 ppm. ³¹P NMR spectra were referenced using an external standard of KPF₆ in D₂O (³¹P δ = -145 ppm vs H₃PO₄ at 0 ppm). Some samples for IR spectroscopy were prepared as KBr pellets and were analyzed on a Nicolet Avatar 370 DTGS (ThermoFisher Scientific, Waltham, MA, USA), while others were analyzed with a Bruker Tensor Standard System spectrometer (ATR) with a range of 4000 to 370 cm⁻¹. High-resolution mass spectra (HR-MS) of 1 and 3 were recorded on an Exactrap mass spectrometer in positive ESI mode (ThermoFisher) with samples injected as acetonitrile solutions. Electrospray MS of 4, 5, 6, 7, and 8 were recorded on a SCIEX 4000 QTRAP hybrid triple quadrupole mass spectrometer in positive ESI mode with samples injected as acetonitrile (4, 5, and 8) and ethanol (6 and 7) solutions. Elemental analyses (C, H, N) were performed by Atlantic Microlab Inc. (Norcross, GA, USA).

Synthesis and Characterization. [Re(CO)₂(Phen)(PTA)Cl] (1). Trimethylamine-*N*-oxide (TMAO, 0.076 g, 0.68 mmol) was dissolved in a mixture of CH₂Cl₂ (200 mL) and CH₃OH (10 mL). A solution of [Re(CO)₃(Phen)(PTA)]⁺ (0.432 g, 0.57 mmol) and NEt₄Cl (1.64 g, 8.91 mmol) in CH₂Cl₂ (180 mL) was heated to reflux at 50 °C, and the TMAO solution was added dropwise over the course of 30 min, changing the color of the solution from light yellow to dark red. The solution was heated under reflux for an additional 24 h. The CH₂Cl₂/CH₃OH was then removed *via* rotary evaporation, and the remaining red solid was suspended in approximately 20 mL of CH₃OH. The solid was isolated by centrifugation and then resuspended in 10 mL of CH₃OH. This process was repeated 3–5 times, yielding the product [Re(CO)₂(Phen)(PTA)Cl] as a red solid. Yield: 0.180 g (51%). ¹H NMR (400 MHz, C₂D₆O₈): δ 9.29 (d, 2H, *J* = 4.9 Hz), 8.86 (d, 2H, *J* = 8.3 Hz), 8.27 (s, 2H), 8.02 (dd, 2H, *J* = 5.0, 8.3 Hz), 4.24 (d, 3H, *J* = 12.8 Hz), 4.10 (d, 3H, *J* = 12.8 Hz), 3.41 (s, 6H). ³¹P{¹H} (162 MHz, C₂D₆O₈; external std, KPF₆): δ -59.19. IR (KBr, cm⁻¹): 1905 s (CO), 1832 s (CO). Anal. Calcd for [Re(CO)₂(Phen)(PTA)Cl] (C₂₀H₂₀ClN₃O₂PRE): C, 39.06; H, 3.28; N, 11.39. Found: C, 38.71; H, 3.34; N, 11.00. HR-ESI-MS (positive ion mode): *m/z* 616.0656 ([M]⁺; calcd, 616.0679).

[Re(CO)₂(Phen)(DAPTA)Cl] (2). Complex 2 was synthesized and characterized as previously described.⁵⁵ All characterization data are in good agreement with previously reported data.

[Re(CO)₂(DMPhen)(PTA)Cl] (3). Trimethylamine-*N*-oxide (TMAO, 0.051 g, 0.46 mmol) was dissolved in a mixture of

CH₂Cl₂ (170 mL) and CH₃OH (7 mL). A solution of [Re(CO)₃(DMPhen)(PTA)]⁺ (0.323 g, 0.41 mmol) and NEt₄Cl (1.18 g, 6.41 mmol) in CH₂Cl₂ (150 mL) was heated to reflux at 50 °C, and the TMAO solution was added dropwise over the course of 30 min, changing the color of the solution from light yellow to dark red. The solution was heated under reflux for an additional 24 h. The CH₂Cl₂/CH₃OH was then removed *via* rotary evaporation, and the remaining red solid was suspended in approximately 20 mL of CH₃OH. The solid was isolated by centrifugation and then resuspended in 10 mL of CH₃OH. This process was repeated 3–5 times, yielding the product as a dark red solid. Yield: 0.204 g (77%). Single crystals of this compound as the dimethylformamide (DMF) solvate were grown by the slow vapor diffusion of diethyl ether into a DMF solution of 3. ¹H NMR (400 MHz, C₂D₆O₈): δ 8.69 (d, 2H, *J* = 8.4 Hz), 8.15 (s, 2H), 8.01 (d, 2H, *J* = 8.4 Hz), 4.17 (d, 3H, *J* = 12.6 Hz), 3.98 (d, 3H, *J* = 12.6 Hz), 3.22 (s, 6H), 3.13 (s, 6H). ³¹P{¹H} (162 MHz, C₂D₆O₈; external std, KPF₆): δ -58.10. IR (KBr, cm⁻¹): 1910 s (CO), 1833 s (CO). Anal. Calcd for [Re(CO)₂(DMPhen)(PTA)Cl] (C₂₂H₂₄ClN₃O₂PRE): C, 41.09; H, 3.76; N, 10.89. Found: C, 40.82; H, 4.02; N, 10.53. HR-ESI-MS (positive ion mode): *m/z* 644.0967 ([M]⁺; calcd, 644.0992).

[Re(CO)₂(DMPhen)(DAPTA)Cl] (4). Trimethylamine-*N*-oxide (0.063 g, 0.57 mmol) was dissolved in a mixture of CH₂Cl₂ (180 mL) and CH₃OH (8 mL). A solution of [Re(CO)₃(DMPhen)(DAPTA)]⁺ (0.405 g, 0.57 mmol) and NEt₄Cl (1.35 g, 7.35 mmol) in CH₂Cl₂ (170 mL) was heated to reflux at 50 °C, and the TMAO solution was added dropwise over the course of 30 min, changing the color of the solution from light yellow to dark red. The solution was heated under reflux for an additional 24 h. The CH₂Cl₂/CH₃OH was then removed *via* rotary evaporation, and the remaining red solid was suspended in approximately 20 mL of CH₃OH. The solid was isolated by centrifugation and then resuspended in 10 mL of CH₃OH. This process was repeated 3–5 times, yielding the product as an orange solid. Crystals were grown from vapor diffusion of diethyl ether into a solution of the complex in DMF. Yield: 0.201 g (60%). For ¹H NMR spectra, DAPTA complexes show the *syn* and *anti* isomers in a 1:5 ratio; however, in the aromatic region the isomers are indistinguishable. ¹H NMR (400 MHz, C₂D₆O₈): δ 8.71 (m, 2H, *anti* + *syn*), 8.21 (m, 2H, *anti* + *syn*), 8.03 (m, 2H, *anti* + *syn*), 5.28 (d, *anti*), 4.80 (d, *syn*), 4.69 (d, *anti*), 4.30 (d, *anti*), 4.04 (m, *syn*), 3.79 (d, *anti*), 3.26 (s, 3H), 3.73 (d, *anti*), 3.10 (m, *anti* + *syn*), 2.62 (d, *anti*), 1.79 (s, *syn*), 1.69 (s, *anti*), 1.38 (s, *anti*). ³¹P{¹H} (162 MHz, C₂D₆O₈; external std, KPF₆): δ -31.06 (*syn*), -32.88 (*anti*). IR (KBr, cm⁻¹): 1906 s (CO), 1827 s (CO). Anal. Calcd for [Re(CO)₂(DMPhen)(DAPTA)Cl] (C₂₅H₂₈ClN₃O₄PRE): C, 41.99; H, 3.95; N, 9.79. Found: C, 41.71; H, 3.99; N, 9.56. ESI-MS (positive ion mode): *m/z* 679.9 ([M - Cl]⁻; calcd, 679.71).

[Re(CO)₂(Phen)(PTA)(H₂O)][NO₃] (5). [Re(CO)₂(Phen)(PTA)(Cl)] (0.100 g, 0.1626 mmol) was dissolved in distilled water (50 mL), and AgNO₃ (0.028 g, 0.1640 mmol) was added to the solution and stirred overnight. The AgCl was filtered off and the filtrate was freeze-dried. Yield: 0.103 g (96%). ¹H NMR (400 MHz, C₂D₆O₈): δ 9.40 (d, 2H, *J* = 5.1 Hz), 9.02 (d, 2H, *J* = 8.3 Hz), 8.38 (s, 2H), 8.16 (dd, 2H, *J* = 5.2, 8.4 Hz), 4.23 (d, 3H, *J* = 13.5 Hz), 4.18 (d, 3H, *J* = 12.9 Hz), 3.52 (s, 6H). ³¹P{¹H} (162 MHz, C₂D₆O₈; external std, KPF₆): δ -69.16. IR (ATR, cm⁻¹): 1905 s (CO), 1829 s (CO). Anal. Calcd For [Re(CO)₂(Phen)(PTA)(H₂O)][NO₃] (C₂₀H₂₂N₆O₃PRE): C, 37.32; H, 3.45; N, 13.06. Found: C, 37.36; H, 3.46; N, 13.09. ESI-MS (positive ion mode): *m/z* 579.6 ([M - H₂O]⁺; calcd, 579.59).

[Re(CO)₂(Phen)(DAPTA)(H₂O)][NO₃] (6). [Re(CO)₂(Phen)(DAPTA)(Cl)] (0.040 g, 0.0582 mmol) was dissolved in distilled water (50 mL), and AgNO₃ (0.010 g, 0.0588 mol) was added to the solution and stirred overnight. The AgCl was filtered off, and the filtrate was freeze-dried. Yield: 0.042 g (99%). ¹H NMR (400 MHz, C₂D₆O₈): δ 9.35 (m, 2H, *anti* + *syn*), 8.89 (d, 2H, *anti* + *syn*), 8.29 (s, 2H, *anti* + *syn*), 8.04 (m, 2H, *anti* + *syn*), 5.35 (d, *anti*), 4.91 (d, *syn*), 4.73 (m, *anti*), 4.50 (dd, *syn*), 4.29 (m, *syn*), 3.95 (dd, *anti*), 3.81 (d, *syn* + *anti*), 3.54 (m, *syn* + *anti*), 3.10 (s, *anti*), 3.04 (s, *syn*), 2.83 (s, *anti*). ³¹P{¹H} (162 MHz, C₂D₆O₈): δ -32.54 (*syn*), -34.63 (*anti*). IR (ATR, cm⁻¹): 1919 s (CO), 1840 s (CO). Anal. Calcd For

[Re(CO)₂(Phen)(DAPTA)(H₂O)][NO₃] (C₂₃H₂₆N₆O₈PRE): C, 37.76; H, 3.58; N, 11.49. Found: C, 37.68; H, 3.56; N, 11.43. ESI-MS (positive ion mode): *m/z* 652.3 ([M - H₂O]⁺; calcd, 652.41).

[Re(CO)₂(DMPhen)(PTA)(H₂O)][NO₃] (7). [Re(CO)₂(DMPhen)(PTA)(Cl)] (0.050 g, 0.0777 mmol) was dissolved in distilled water (50 mL) and AgNO₃ (0.0132 g, 0.0777 mmol) was added to the solution and stirred overnight. The AgCl was filtered off, and the filtrate was freeze-dried. Yield: 0.053 g (99%). ¹H NMR (400 MHz, C₂D₆OS): δ 8.85 (d, 1H, *J* = 8.4 Hz), 8.68 (d, 1H, *J* = 8.4 Hz), 8.26 (s, 2H), 8.18 (s, 1H), 8.15 (s, 1H), 7.99 (d, 1H, *J* = 8.4 Hz), 4.15 (d, 2H, *J* = 13.2 Hz), 3.96 (d, 2H, *J* = 13.2 Hz), 3.51 (s, 4H), 3.29 (2, 4H), 3.25 (s, 3H), 3.13 (s, 3H). ³¹P {¹H} (162 MHz, C₂D₆OS): δ -58.71. IR (ATR, cm⁻¹): 1909 s (CO), 1828 s (CO). Anal. Calcd For [Re(CO)₂(DMPhen)(PTA)(H₂O)][NO₃] (C₂₂H₂₆N₆O₆PRE): C, 38.42; H, 3.81; N, 12.22. Found: C, 38.21; H, 3.79; N, 12.24. ESI-MS (positive ion mode): *m/z* 608.2 ([M - H₂O]⁺; calcd, 608.41).

[Re(CO)₂(DMPhen)(DAPTA)(H₂O)][NO₃] (8). [Re(CO)₂(DMPhen)(DAPTA)(Cl)] (0.100 g, 0.140 mmol) was dissolved in distilled water (50 mL), and AgNO₃ (0.024 g, 0.141 mmol) was added to the solution and stirred overnight. The AgCl was filtered off and the filtrate was freeze-dried. Yield: 0.100 g (94%). ¹H NMR (400 MHz, D₂O): δ 8.63 (d, 2H, *anti* + *syn*), 8.09 (s, 2H, *anti* + *syn*), 7.98 (m, 2H, *anti* + *syn*), 5.39 (d, *anti*), 4.97 (d, *syn*), 4.88 (d, *anti*), 4.33 (d, *anti* + *syn*), 3.85 (m, *anti* + *syn*), 3.41 (d, *anti* + *syn*), 3.33 (s, 6H), 3.07 (d, *syn*), 2.97 (m, *anti*), 2.80 (d, *anti*), 1.94 (s, *syn*), 1.85 (s, *anti*), 1.47 (s, *anti*). ³¹P {¹H} (162 MHz, D₂O): δ -26.8 (*anti*), -29.6 (*syn*). IR (ATR, cm⁻¹): 1915 s (CO), 1830 s (CO). Anal. Calcd For [Re(CO)₂(DMPhen)(DAPTA)(H₂O)][NO₃] (C₂₃H₂₆N₆O₈PRE): C, 39.42; H, 4.23; N, 11.03. Found: C, 39.36; H, 4.21; N, 11.00. ESI-MS (positive ion mode): *m/z* 721.9 ([M - H₂O + CH₃CN]⁺; calcd, 721.77).

X-ray Crystallography. Low-temperature (100 K) X-ray diffraction data for 4 was collected on a Rigaku XtaLab Synergy diffractometer equipped with a four-circle Kappa goniometer and HyPix 6000HE Hybrid Photon Counting (HPC) detector with monochromated Mo K α radiation (λ = 0.71073 Å). Diffraction images were processed using CrysAlisPro software.⁶² Low-temperature diffraction (223 K) data for 3a were collected on a Bruker X8 Kappa diffractometer coupled to an ApexII CCD detector with monochromated Mo K α radiation. The structure was solved through intrinsic phasing using SHELXT⁶³ and refined against *F*² on all data by full-matrix least-squares with SHELXL⁶⁴ following established strategies.⁶⁵ All non-hydrogen atoms were refined anisotropically. Hydrogen atoms were included in the model at geometrically calculated positions and refined using a riding model, while allowing the torsion angle to refine using the appropriate HFIX command. The isotropic displacement parameters of these hydrogen atoms were set to 1.2 times that of the atom which they are bound to (1.5 times the carbon atom that for methyl groups). Details of the structure refinement and selected interatomic distances and angles can be found in the crystallographic data on the CSD.

Kinetic Studies. All of the reactions were studied at pH = 5.00 using HNO₃. For aquation studies, the correct masses of 1–4 were dissolved in 1 mL of DMF dissolved and diluted with water containing NaClO₄ so that the final concentrations of 1–4 were 0.015, 0.05, 0.015, and 0.05 mM, respectively, and their ionic strength was either 0.015, 1, or 2 M, under aerobic conditions. The absorbances at selected wavelengths were then recorded at different time intervals. These data were fitted to the first-order rate equation (eq 1), giving the *k*_{obs} values for each aquation.

$$A_t = A_\infty - (A_\infty - A_0)e^{-k_{\text{obs}}t} \quad (1)$$

$$k_{\text{obs}} = k_{\text{Cl}}[\text{Cl}^-] + k_{\text{aq}} \quad (2)$$

The anation reactions of 5–8 were measured aerobically under *pseudo*-first-order conditions with chloride ions in large excess, ranging from 0.1 to 1 M at various ionic strengths and temperatures. The ligand was in excess in each case, and the metal concentration

was kept constant. Each kinetic run was performed at least twice, and an average of the values was used.

The *pseudo*-first-order rate constant (*k*_{obs}) is determined by a least-squares fit of the absorbance vs time data for the reaction to eq 1. This equation was used in all of the kinetic runs. The concentration dependence of *k*_{obs} for the anation reactions at pH = 5.00 were observed as straight lines and *k*_{Cl} (anation) and *k*_{aq} (aquation) could be calculated from the slopes and intercepts, respectively, by fitting the data to eq 2.

Equilibrium Studies. The stability constant, *K*, could be calculated by eq 3.

$$K = k_{\text{Cl}}/k_{\text{aq}} \quad (3)$$

K was also determined spectrophotometrically under equilibrium conditions from a plot of absorption vs [Cl⁻] using eq 4, where *A*_{aq} and *A*_{Cl} are the observed absorbance of the aqua and the chlorido complexes, respectively.

$$A_t = (A_{\text{aq}} + A_{\text{Cl}}K[\text{Cl}^-]) / (1 + K[\text{Cl}^-]) \quad (4)$$

Acid Dissociation Constants. The acid dissociation constants of 5–8 were determined spectrophotometrically at 25.0 °C and at the corresponding wavelengths, 360, 360, 275, and 360 nm. In a typical experiment the pH of a 0.03–0.2 mM solution of the aqua complex was adjusted from pH ~4 to ~11 with sodium hydroxide (aqueous solutions from 1 × 10⁻⁶ to 1 × 10⁻² M from a 1.0 M stock solution). The absorbance was measured at various time points over a 3 h period. The ionic strength was kept constant at 1 M with NaClO₄. No evidence was found for time-dependent changes on variation of the pH in the time frames of our experimental work, indicating that the formation of the hydroxo bridged complexes could be excluded. The absorbance vs pH data were fitted to eq 5 (where Abs is the observed absorbance at a specific pH, *A*_H is the absorbance of the protonated species, *A*₀ is the absorbance of the deprotonated species, and *K*_{a1} is the acid dissociation constant), and the resultant p*K*_a values are reported in Table 1.

$$\text{Abs} = \{A_{\text{H}} + A_0(K_{\text{a1}}/[\text{H}^+])\} \div \{1 + (K_{\text{a1}}/[\text{H}^+])\} \quad (5)$$

Table 1. Calculated p*K*_a Values for Complexes 5–8

complex	p <i>K</i> _a
5	9.28 ± 0.03
6	9.21 ± 0.03
7	9.12 ± 0.09
8	9.09 ± 0.03

RESULTS

Synthesis and Characterization. The Re(I) dicarbonyl complexes were synthesized from their tricarbonyl precursors, following a previously reported procedure.⁶⁶ Briefly, the Re(I) tricarbonyl phosphine complexes were treated with trimethylamine-*N*-oxide, an oxygen atom donor that is commonly used to oxidize CO from transition metal complexes. The CO ligand trans to the phosphine is selectively displaced by this reaction as it leaves in the form of CO₂. The subsequent treatment of the resulting dicarbonyl complex with an excess of [NEt₄][Cl] affords the respective [Re(CO)₂(NN)(PR₃)(Cl)] complex. The axial chlorido can be removed in a subsequent step using AgNO₃ to obtain the cationic aqua complex, [Re(CO)₂(NN)(PR₃)(OH₂)]⁺. For this study, eight Re(I) dicarbonyl phosphine complexes bearing an equatorial Phen or DMPhen ligand were synthesized. The choice of equatorial ligands was motivated by the previously observed high cytotoxicity of the Re(I) tricarbonyl complexes bearing both the Phen and DMPhen ligands. The use of PTA and DAPTA as phosphine ligands provides an interesting opportunity to compare these

complexes, as the PTA complexes were previously found to be inactive under conditions of photoirradiation.

All eight of the complexes were characterized by standard spectroscopic techniques. Notably, only two CO stretching modes are observed in the IR spectra of these complexes, in contrast to the three that are detected for the tricarbonyl precursors. Additionally, the energies of the dicarbonyl stretching modes ($\sim 1825\text{--}1930\text{ cm}^{-1}$) in **1–8** are significantly lower than those for the tricarbonyl precursors ($\sim 1910\text{--}2040\text{ cm}^{-1}$). The lower energy CO stretches of the dicarbonyl species are expected because the back-donation of the Re(I) electrons is now only distributed over two CO ligands.

X-ray Crystallography. Single crystals of $[\text{Re}(\text{CO})_2(\text{DMPhen})(\text{PTA})(\text{Cl})]\cdot\text{DMF}$ (**3a**) and $[\text{Re}(\text{CO})_2(\text{DMPhen})(\text{DAPTA})(\text{Cl})]$ (**4**) were obtained, and their crystal structures (Figure 2 and Table 2) were determined by X-ray crystallography.

The asymmetric unit for **3a** consists of a full molecule and one solvent DMF molecule, whereas, for **4**, only the complex comprises the asymmetric unit. Both complexes exhibit the expected octahedral geometry with the central rhenium atom surrounded by the bidentate ligand, two carbonyl ligands, and

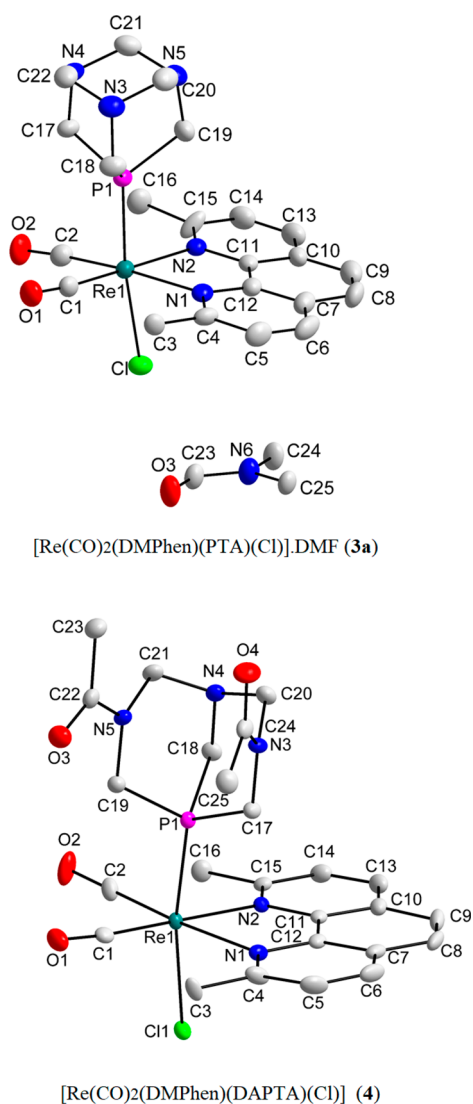


Figure 2. Graphical illustration of the crystal structures of **3a** and **4**.

Table 2. Crystallographic Data of **3a** and **4**

	3a	4
empirical formula	C ₂₅ H ₃₁ ClN ₆ O ₃ PRe	C ₂₅ H ₂₆ ClN ₅ O ₄ PRe
FW (g mol ⁻¹)	716.18	715.14
cryst syst	monoclinic	monoclinic
space group	Cc	P2 ₁ /c
a (Å)	19.6656(13)	13.7728(2)
b (Å)	11.8373(7)	8.7908(2)
c (Å)	11.4246(7)	21.2310(4)
α (deg)	90	90
β (deg)	90.679(3)	94.638(2)
γ (deg)	90	90
Z	4	4
cryst color	orange-yellow	orange-yellow
temp (K)	296(2)	100(2)
R _{int}	0.0285	0.0421
GooF	1.005	1.042
R [I > 2σ(I)]		
R ₁	0.0245	0.0207
R _{w2}	0.0488	0.0477
R (all data)		
R ₁	0.0268	0.0244
R _{w2}	0.0499	0.0487

the phosphine ligand trans to a chlorido ligand. These structures provide conclusive verification that the displaced CO was removed selectively from the position trans to the phosphine. The Re–Cl bond distances for both of these complexes are quite similar (2.4922(6) Å and 2.4991(13) Å), but the Re–P bonding distance of **4** is slightly shorter than that of **3** (2.3072(7) Å vs 2.3227(14) Å).

The P–Re–Cl angles are 172.56(5)° and 170.31(2)° for **3a** and **4**, respectively, indicating the slightly distorted geometry of both complexes. All of the bond distances and angles correspond well with other structures in literature and are considered normal. Selected bond lengths and angles of the crystal structures of **3a** and **4** are given in Table 3. The DAPTA

Table 3. Selected Bond Lengths and Angles of the Structures of **3a** and **4**

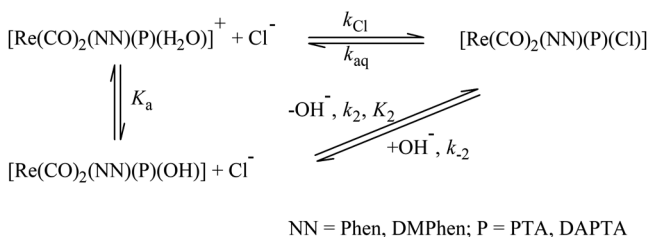
bond length/angle	3a	4
Re1–C1	1.880(5) Å	1.893(3)
Re1–C2	1.889(6) Å	1.881(3) Å
Re1–P1	2.3227(14) Å	2.3072(7) Å
Re1–Cl1	2.4991(13) Å	2.4922(6) Å
Re1–N1	2.232(5) Å	2.231(2) Å
Re1–N2	2.247(4) Å	2.226(2) Å
N1–Re1–N2	75.61(16)°	75.60(8)°
P1–Re1–Cl1	172.56(5)°	170.31(2)°

ligand of **4** crystallized as the *anti* isomer, whereby the acetate groups are oriented in different directions. By NMR spectroscopy, the *anti* isomer was also found to be the major species in solution.⁵⁵

Both crystal structures are stabilized by inter- and intramolecular interactions (see Table S1 and Figure S1 in the Supporting Information (SI) for discussion and illustration).

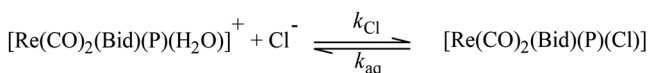
Kinetics. Scheme 1 represents the anation and protonation of **5–8** by chloride ions in water. Herein K_a is the acid dissociation constant of the respective aqua complexes. The

Scheme 1. Schematic Representation of the Aqueous Protonation and Aqua Substitution of $[\text{Re}(\text{CO})_2(\text{Bid})(\text{P})(\text{H}_2\text{O})]^+$ Type Complexes by Chloride Ions (Bid = Phen, DMPhen; P = PTA, DAPTA)



$\text{p}K_{\text{a}1}$ values of 5–8 are all >9 (Table 1). On the basis of these data, it can be deduced that deprotonation of the aqua products is negligible at $\text{pH} = 5.00$ and that Scheme 1 can be simplified to a single-step, reversible reaction as depicted in Scheme 2.

Scheme 2. Simplified Mechanism for the Aqua Substitution in $[\text{Re}(\text{CO})_2(\text{Bid})(\text{P})(\text{H}_2\text{O})]^+$ Type Complexes, at $\text{pH} 5$



Under *pseudo*-first-order conditions, plots of k_{obs} vs $[\text{Cl}^-]$ should give a slope = k_{Cl} and an intercept = k_{aq} .⁴⁴ The k_{obs} vs $[\text{Cl}^-]$ plots of aqueous solutions of 5–8 at 298 K and at 1 M NaClO_4 are shown in the Supporting Information (Tables S2–S9 and Figures S2–S5). The presence of isosbestic points indicates a single-step reaction, the conversion of chlorido species to the aqua products, thereby confirming that Scheme 2 is a correct representation of the reaction at $\text{pH} = 5.0$.

Taking the above into consideration, the aquation reactions of 1–4 were studied at 298 K at various ionic strengths (0.015–2 M NaClO_4). The observed rate constants are given in Table 4. It is clear that the ionic strength range employed here has no significant effect on the reaction rates. These data enabled us to follow the aquation of 1–4 also at 288, 308, and 318 K in a consistent ionic strength of 1 M NaClO_4 (Table 4). Figure 3 illustrates the UV/vis spectral change and the absorbance vs time plot for the aquation of complex 4.

The anation reactions of 5–8 were studied at four temperatures (288, 298, 308, and 318 K) at an ionic strength of 1 and 2 M NaClO_4 at 298 K (Table 5). The values of k_{aq} agree very well with the intercept of the reverse anation reactions, giving further proof that the reaction presented in Scheme 2 is correct and that k_{aq} could also be calculated from the anation reaction data. Figure 4a illustrates the k_{obs} vs $[\text{Cl}^-]$ data for the reaction between 5 and the chloride ions at 15.0–45.0 °C and $[\text{NaClO}_4] = 1$ M. Figure 4b illustrates the k_{obs} vs $[\text{Cl}^-]$ data for 6, 7, and 8 at 25.0 °C. The k_{obs} vs $[\text{Cl}^-]$ plots of 6, 7, and 8 are given in the Supporting Information (Figures S3–S5).

The aquation reactions of the Phen complexes (1 and 2) are about 2.5 times faster than those of the DMPhen complexes (3 and 4) at 298 K. Similarly, the anation rate constants (k_{Cl}) are about two times slower for the DMPhen complexes at 298 K. The values of the equilibrium constants were calculated from the ratios of $k_{\text{aq}}/k_{\text{Cl}}$ and also confirmed by spectrophotometric determination (K_{spec} in Table 5) (summarized in Table S10 in the Supporting Information).

Table 4. Summary of the Observed Rate Constants (k_{aq}) for the Aquation Reactions of 1–4 at Different Ionic Strengths and Temperatures

compd	$[\text{NaClO}_4]$ (M)	T (K)	k_{aq} (10^{-4} s^{-1})	
1	1	288	4.37 ± 0.05	
	1	298	12.5 ± 0.7	
	1	308	31.1 ± 0.6	
	1	318	73.0 ± 1.1	
	0.015	298	13.0 ± 0.6	
	2	298	12.1 ± 0.8	
	2	1	288	5.32 ± 0.4
		1	298	15.7 ± 0.3
		1	308	34 ± 1
		1	318	85 ± 12
0.015		298	12.7 ± 0.5	
2		298	13 ± 1	
3		1	288	1.3 ± 0.3
		1	298	3.7 ± 0.3
		1	308	13 ± 1
		1	318	29 ± 3
	0.015	298	4.1 ± 0.6	
	2	298	4.9 ± 0.3	
	4	1	288	1.65 ± 0.05
		1	298	4.01 ± 0.04
		1	308	11.1 ± 0.08
		1	318	24.5 ± 0.5
0.015		298	4.18 ± 0.06	
2		298	4.04 ± 0.04	

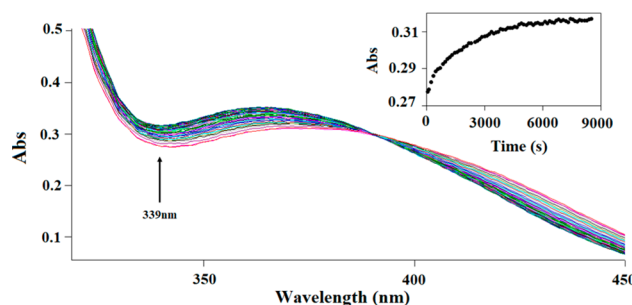


Figure 3. Illustration of the UV/vis spectral change of the aquation of 4 and the absorbance vs time data at 339 nm, $\text{pH} = 5$, $[\text{Re}] = 5.0 \times 10^{-5}$ M, and $[\text{NaClO}_4] = 1$ M.

The rate constants of both the anation and aquation reactions were also studied at different temperatures so that the activation enthalpy (ΔH^\ddagger) and activation entropy (ΔS^\ddagger) could be calculated from the Arrhenius equation. The values of ΔS^\ddagger are negative for all eight complexes (Table 6).

DISCUSSION

The rate constants for aquation of the chloride complexes (1–4) are mostly independent of the ionic strength. The anation reaction, however, shows a slight dependence on the ionic strength, with decreasing rate constants at higher ionic strengths. This result is in agreement with the Bronsted equation, which shows that higher ionic strength solutions slow down chemical reactions between species of opposite charges.⁶⁷ The high negative values of ΔS^\ddagger suggest associative pathways for both the anation and aquation processes.

The first-order rate constant for water exchange of *fac*- $[\text{Re}(\text{CO})_3(\text{H}_2\text{O})]^+$ was reported as $(6.3 \pm 0.1) \times 10^{-3} \text{ s}^{-1}$ at

Table 5. Summary of the Kinetic Data for the Anation Reactions of 5–8, at Different Ionic Strengths and Temperatures

compd	[NaClO ₄] (M)	T (K)	$k_{\text{Cl}} (10^{-3}) (M^{-1} s^{-1})$	$k_{\text{aq}} (10^{-4}) (s^{-1})$	$K_{\text{Cl}} (M^{-1})$	K_{spec}
5	1	288	2.15 ± 0.04	5.2 ± 0.6	4.1 ± 0.5	5 ± 1
	1	298	6.40 ± 0.07	14.1 ± 0.7	4.5 ± 0.2	
	1	308	19.5 ± 0.6	35 ± 9	5.6 ± 1.4	
	1	318	55 ± 2	71 ± 2	7.7 ± 0.4	
	2	298	4.92 ± 0.7	14.3 ± 0.9	3.4 ± 0.2	
6	1	288	2.16 ± 0.03	3.5 ± 0.4	6.2 ± 0.7	4.4 ± 0.9
	1	298	6.79 ± 0.09	10 ± 1	6.8 ± 0.7	
	1	308	24.2 ± 0.4	24 ± 4	10 ± 2	
	1	318	70.3 ± 0.9	65 ± 6	11 ± 1	
	2	298	4.58 ± 0.09	14 ± 1	3.9 ± 0.3	
	2	298	4.58 ± 0.09	14 ± 1	3.9 ± 0.3	
7	1	288	0.93 ± 0.01	1.1 ± 0.3	8 ± 2	4.5 ± 0.7
	1	298	3.16 ± 0.09	3.4 ± 0.1	9.3 ± 0.4	
	1	308	9.9 ± 0.4	12.0 ± 0.6	8.3 ± 0.4	
	1	318	26 ± 2	28 ± 3	9 ± 1	
	2	298	2.3 ± 0.9	4.1 ± 0.6	7 ± 2	
8	1	288	0.773 ± 0.008	1.3 ± 0.5	6 ± 2	4.3 ± 0.6
	1	298	2.99 ± 0.05	3.6 ± 0.3	8.3 ± 0.7	
	1	308	8.72 ± 0.09	9.3 ± 0.5	9.4 ± 0.5	
	1	318	24 ± 1	29 ± 2	8.3 ± 0.7	
	2	298	2.1 ± 0.2	3.5 ± 0.8	7 ± 2	

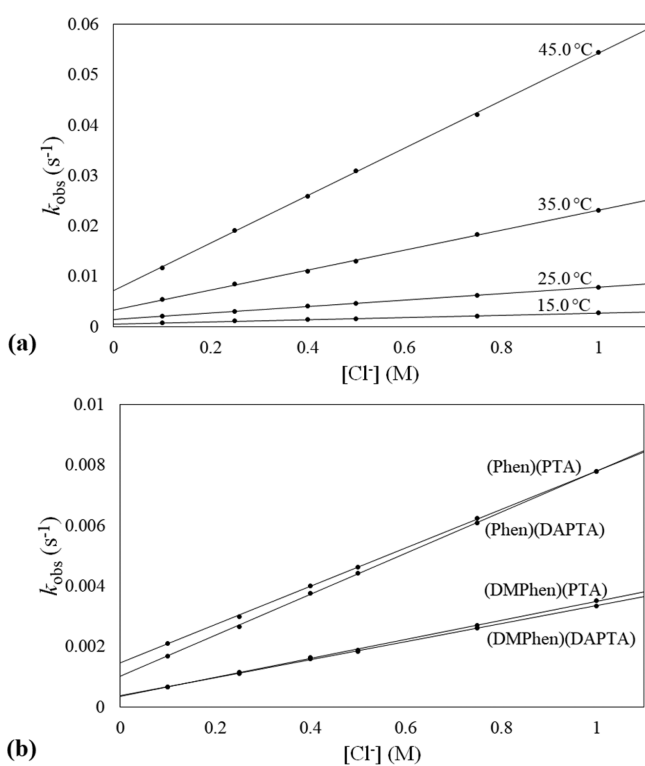


Figure 4. (a) Plot of k_{obs} vs $[\text{Cl}^-]$ for the reaction between **1** ($[\text{Re}] = 2.5 \times 10^{-5} \text{ M}$; $\lambda = 269 \text{ nm}$) and chloride ions, at different temperatures; (b) plot of k_{obs} vs $[\text{Cl}^-]$ for the reaction between **1** ($[\text{Re}] = 2.5 \times 10^{-5} \text{ M}$; $\lambda = 269 \text{ nm}$), **3** ($[\text{Re}] = 5 \times 10^{-5} \text{ M}$; $\lambda = 269 \text{ nm}$), **2** ($[\text{Re}] = 2.5 \times 10^{-4} \text{ M}$; $\lambda = 360 \text{ nm}$), and **4** ($[\text{Re}] = 2.5 \times 10^{-4} \text{ M}$, $\lambda = 339 \text{ nm}$) and chloride ions at 25.0 °C. pH = 5; $[\text{NaClO}_4] = 1 \text{ M}$.

298 K.⁶⁸ This value is very similar to the rates of anation, k_{Cl} , for 5–8. This result is more suggestive of an I_{d} type of activation as expected for most octahedral complexes.

The rate constants for aquation of the Phen complexes are greater than those of the respective DMPhen counterparts.

Table 6. Activation Parameters for the Aquation of Complexes 1–4 and the Anation of Complexes 5–8

complex	$\Delta H^\ddagger (\times 10^3 \text{ kJ mol}^{-1})$	$\Delta S^\ddagger (\text{J K}^{-1} \text{ mol}^{-1})$
1	68 ± 1	−69 ± 3
2	67 ± 2	−75 ± 8
3	78 ± 4	−68 ± 8
4	69 ± 2	−76 ± 6
5	82.6 ± 0.9	−9 ± 2
6	82.1 ± 0.9	−10 ± 3
7	82 ± 2	−16 ± 5
8	82.6 ± 0.5	−16 ± 3

The same trend is seen for the anation reactions. This result implies that bond breaking alone is not rate determining and would suggest an associative I_{a} type mechanism. Furthermore, the Re–Cl bond distances for **3a** and **4** are nearly identical (2.4991(13) Å and 2.4922(6) Å, respectively) and slightly shorter than the distance reported for **1** earlier (2.5018(9) Å);⁵⁵ however, the rates of hydrolysis of the DMPhen complexes are more than 2.5 times slower than the corresponding Phen complexes. This hypothesis is further supported by the negative values for the activation entropy. In general, one would expect that the steric bulk of the DMPhen ligand would hinder the association of an entering ligand in an I_{a} type mechanism, slowing down the reaction rate, as is found here.

The phosphine ligand itself does not seem to greatly influence either aquation or anation of these complexes, with the DAPTA complexes reporting slightly faster rates in general.

As mentioned above, the speciation of the complexes in various biological conditions can be predicted (Table 7) by using the equilibrium constant data for the aquation reactions of the chlorido complexes. As indicated in Table 5, complexes 5–8 all have equilibrium constants in the region of 5 M^{-1} at 298 K and even at 308 K, which is closer to the human body temperature. Also, since the $\text{p}K_{\text{a}}$ values of all four of the aqua complexes are very similar, the general value of $K_{\text{Cl}} = 5.0 \text{ M}^{-1}$ and $\text{p}K_{\text{a}} = 9.28$ can be used (see the SI for calculations).

Table 7. Speciation of Rhenium Complexes in Blood Plasma, The Cell Cytoplasm, and the Nucleus at pH = 7.4, 298 K, and $K_{Cl} = 5 \text{ M}^{-1}$

	$[\text{Cl}^-]$ (mM)	Re–Cl (%)	Re–H ₂ O (%)	Re–OH (%)
plasma	104	2.04	96.69	1.27
cytoplasm	22.7	0.45	98.26	1.29
nucleus	4	0.08	98.63	1.29

The $[\text{Cl}^-]$ in blood plasma is higher (104 mM) than in the cell cytoplasm (22.7 mM) and cell nucleus (4 mM). On the basis of the equilibrium constant data, however, the major species in all three of these biological environments would be the rhenium aqua complexes. Very small amounts of the hydroxo and chlorido species are predicted to exist within any of these environments. It is common knowledge that metal–hydroxo species are highly unreactive toward substitution, so one would expect that these species would not react with biological substrates.^{44,69,70} On the other hand, the aqua complexes are monocationic which should improve their cellular uptake in comparison to their neutral chlorido and hydroxido derivatives.

These results differ substantially from cisplatin for which the percentage of unreactive dihydroxo forms are more or less similar to the diaqua species (35%).⁷¹ This affects the dosage value since more of the drug has to be administered in order to obtain enough of the active species.

The cell toxicities of **2** and **5** were reported previously.⁵⁵ The PTA complex (**5**) was nontoxic in HeLa cells up to 200 μM in the dark, whereas the DAPTA complex showed mild cytotoxicity at concentrations $> 50 \mu\text{M}$. On the basis of the information above, one would expect that both **2** and **5** are rapidly hydrolyzed to form their aqua analogues. The enhanced cytotoxic activity of **6**, in this case, can thus be attributed to the DAPTA ligand.

It is clear from these data that the aqua species are at least 10 times more reactive than their respective chlorido species and would easily bind to proteins, as was shown recently for a similar tricarbonyl counterpart.⁷²

CONCLUSION

The aquation reactions of four different Re(I) dicarbonyl complexes bearing a water-soluble phosphine ligand trans to the leaving Cl^- have been investigated. The data mostly suggest an I_a type mechanism, a conclusion that is further supported by the slower reaction rates for complexes bearing the bulkier DMPhen ligand. It will be important to perform high-pressure kinetic studies to further validate the intimate mechanism for the substitution reactions of this class of compounds. More importantly, the 2-fold difference in rate between the Phen and Dapta complexes suggests that variations in electronic and steric effects of the bidentate ligands modulate the aquation rate. The fact that the anation reactions are about 10 times faster than the respective aquation reactions results in equilibrium constants for hydrolysis ranging from 4.5 to 9.3 M^{-1} .

Importantly, the pK_a studies show that the aqua forms of **1–4** are the major species in blood plasma, cell cytoplasm, and the nucleus, as opposed to unreactive hydroxo species. This is different from what was found for *cis*-platin and ruthenium(II) arene complexes where hydroxo species are prevalent.^{57,73}

Presumably, the resulting positively charged complexes will be taken up by cells and mitochondria more effectively than

conventional Re(I) tricarbonyl complexes. Furthermore, the pK_a of these complexes is such that negligible amounts of hydroxo are expected to be present at physiologically relevant pH. Thus, these complexes will still be able to form covalent adducts with proteins or other biological targets. Although several of these dicarbonyl complexes were not highly cytotoxic, this class of compounds offers exciting prospects for future research, as larger libraries of these compounds have not yet been subjected to thorough biological studies. The data presented in this work provide a guide for researchers pursuing the biological properties of this class of compounds. We have shown, for example, how modifying the steric environment of these complexes can rationally modify the observed aquation kinetics. The results from this study are of importance for aspects related to synthesis, *in vivo* stability, and uptake and excretion of dicarbonyl complexes of rhenium(I). We anticipate that rhenium(I) dicarbonyl complexes will comprise an interesting class of anticancer agents within the near future.

ASSOCIATED CONTENT

Supporting Information

The Supporting Information is available free of charge at <https://pubs.acs.org/doi/10.1021/acs.inorgchem.0c02389>.

Extra crystallographic and kinetic data (PDF)

Accession Codes

CCDC 2019299 and 2019300 contain the supplementary crystallographic data for this paper. These data can be obtained free of charge via www.ccdc.cam.ac.uk/data_request/cif, or by emailing data_request@ccdc.cam.ac.uk, or by contacting The Cambridge Crystallographic Data Centre, 12 Union Road, Cambridge CB2 1EZ, UK; fax: +44 1223 336033.

AUTHOR INFORMATION

Corresponding Author

Hendrik G. Visser – Department of Chemistry, University of the Free State, Bloemfontein, South Africa 9301; Email: visserhg@ufs.ac.za

Authors

Marietjie Schutte-Smith – Department of Chemistry, University of the Free State, Bloemfontein, South Africa 9301; orcid.org/0000-0001-8935-7601

Sierra C. Marker – Department of Chemistry and Chemical Biology, Cornell University, Ithaca, New York 14853, United States

Justin J. Wilson – Department of Chemistry and Chemical Biology, Cornell University, Ithaca, New York 14853, United States; orcid.org/0000-0002-4086-7982

Complete contact information is available at: <https://pubs.acs.org/doi/10.1021/acs.inorgchem.0c02389>

Notes

The authors declare no competing financial interest.

ACKNOWLEDGMENTS

We thank the University of the Free State and the NRF for funding, as well as Joshua J. Woods for the data collection and Tracky Huang for assistance in the laboratory.

REFERENCES

(1) Siegel, R. L.; Miller, K. D.; Jemal, A. Cancer Statistics, 2017. *Ca-Cancer J. Clin.* **2017**, *67*, 7–30.

- (2) Lippert, B. E. *Cisplatin: Chemistry and Biochemistry of a Leading Anticancer Drug*; Wiley-VCH: Zurich, Switzerland, 1999.
- (3) Meijer, C.; Mulder, N. H.; Timmer-Bosscha, H.; Sluiter, W. J.; Meersma, G. J.; de Vries, E. G. Relationship of Cellular Glutathione to the Cytotoxicity and Resistance of Seven Platinum Compounds. *Cancer Res.* **1992**, *52* (24), 6885–6889.
- (4) Summa, N.; Schiessl, W.; Puchta, R.; van Eikema Hommes, N.; van Eldik, R. Thermodynamic and Kinetic Studies on Reactions of Pt(II) Complexes with Biologically Relevant Nucleophiles. *Inorg. Chem.* **2006**, *45*, 2948–2959.
- (5) Galanski, M. A.; Jakupec, M.; Keppler, B. K. Update of the Preclinical Situation of Anticancer Platinum Complexes: Novel Design Strategies and Innovative Analytical Approaches. *Curr. Med. Chem.* **2005**, *12*, 2075–2094.
- (6) Li, J.; Chen, F.; Cona, M. M.; Feng, Y.; Himmelreich, U.; Oyen, R.; Verbruggen, A.; Ni, Y. A Review on Various Targeted Anticancer Therapies. *Target. Oncol.* **2012**, *7*, 69–85.
- (7) Johnstone, T. C.; Suntharalingam, K.; Lippard, S. J. Third Row Transition Metals for the Treatment of Cancer. *Philos. Trans. R. Soc., A* **2015**, *373*, 20140185.
- (8) Marloye, M.; Berger, G.; Gelbcke, M.; Dufrasne, F. A Survey of the Mechanisms of Action of Anticancer Transition Metal Complexes. *Future Med. Chem.* **2016**, *8*, 2263–2286.
- (9) Peana, M. F.; Medici, S.; Zoroddu, M. A. The Intriguing Potential of “Minor” Noble Metals: Emerging Trends and New Applications. *Biomedical Applications of Metals*; Rai, M., Ingle, A. P., Medici, S., Eds.; Springer: Cham, Switzerland, 2018; Vol. 221, pp 49–72, DOI: 10.1007/978-3-319-74814-6_2.
- (10) Meggers, E. Targeting Proteins with Metal Complexes. *Chem. Commun.* **2009**, 1001–1010.
- (11) Manav, N.; Kesavan, P. E.; Ishida, M.; Mori, S.; Yasutake, Y.; Fukatsu, S.; Furuta, H.; Gupta, I. Phosphorescent Rhenium-dipyridinates: Efficient Photosensitizers for Singlet Oxygen Generation. *Dalton Trans.* **2019**, *48*, 2467–2478.
- (12) Thorp-Greenwood, F. L.; Pritchard, V. E.; Coogan, M. P.; Hardie, M. J. Tris(rhenium *fac*-tricarbonyl) Polypyridine Functionalized Cyclotriguanaicylene Ligands with Rich and Varied Emission. *Organometallics* **2016**, *35*, 1632–1642.
- (13) Ramos, L. D.; Sampaio, R. N.; De Assis, F. F.; De Oliveira, K. T.; Homem-De-Mello, P.; Patrocínio, A. O. T.; Frin, K. P. M. Contrasting Photophysical Properties of Rhenium(I) Tricarbonyl Complexes Having Carbazole Groups Attached to the Polypyridine Ligand. *Dalton Trans.* **2016**, *45*, 11688–11698.
- (14) Bauer, E. B.; Haase, A. A.; Reich, E. M.; Crans, D. C.; Kühn, F. E. Organometallic and Coordination Rhenium Compounds and their Potential in Cancer Therapy. *Coord. Chem. Rev.* **2019**, *393*, 79–117.
- (15) Haase, A. A.; Bauer, E. B.; Kühn, F. E.; Crans, D. C. Speciation and Toxicity of Rhenium Salts, Organometallics and Coordination Complexes. *Coord. Chem. Rev.* **2019**, *394*, 135–150.
- (16) Sato, D.; Ishitani, O. Photochemical Reactions of *fac*-Rhenium(I) Tricarbonyl Complexes and their Application for Synthesis. *Coord. Chem. Rev.* **2015**, *282–283*, 50–59.
- (17) Gómez-Iglesias, P.; Guyon, F.; Khatyr, A.; Ulrich, G.; Knorr, M.; Martín-Alvarez, J. M.; Miguel, D.; Villafañe, F. Luminescent Rhenium(I) Tricarbonyl Complexes with Pyrazolylamidino Ligands: Photophysical, Electrochemical, and Computational Studies. *Dalton Trans.* **2015**, *44*, 17516–17528.
- (18) Konkankit, C. C.; Marker, S. C.; Knopf, K. M.; Wilson, J. J. Anticancer Activity of Complexes of the Third Row Transition Metals, Rhenium, Osmium, and Iridium. *Dalton Trans.* **2018**, *47*, 9934–9974.
- (19) Viguri, M. E.; Pérez, J.; Riera, L. C-C Coupling of N-Heterocycles at the *fac*-Re(CO)₃ Fragment: Synthesis of Pyridylimidazole and Bipyridine Ligands. *Chem. - Eur. J.* **2014**, *20*, 5732–5740.
- (20) Gantsho, V. L.; Dotou, M.; Jakubaszek, M.; Goud, B.; Gasser, G.; Visser, H. G.; Schutte-Smith, M. Synthesis, Characterization, Kinetic Investigation and Biological Evaluation of Re(I) Di- and Tricarbonyl Complexes with Tertiary Phosphine Ligands. *Dalton Trans.* **2020**, *49*, 35–46.
- (21) Knopf, K. M.; Murphy, B. L.; MacMillan, S. N.; Baskin, J. M.; Barr, M. P.; Boros, E.; Wilson, J. J. *In Vitro* Anticancer Activity and *In Vivo* Biodistribution of Rhenium(I) Tricarbonyl Aqua Complexes. *J. Am. Chem. Soc.* **2017**, *139*, 14302–14314.
- (22) Popov, D. A.; Luna, J. M.; Orchanian, N. M.; Haiges, R.; Downes, C. A.; Marinescu, S. C. A 2,2'-Bipyridine-containing Covalent Organic Framework Bearing Rhenium(I) Tricarbonyl Moieties for CO₂ Reduction. *Dalton Trans.* **2018**, *47*, 17450–17460.
- (23) Maurin, A.; Ng, C.-O.; Chen, L.; Lau, T.-C.; Robert, M.; Ko, C.-C. Photochemical and Electrochemical Catalytic Reduction of CO₂ with NHC-containing Dicarboxyl Rhenium(I) Bipyridine Complexes. *Dalton Trans.* **2016**, *45*, 14524–14529.
- (24) Matlachowski, C.; Braun, B.; Tschierlei, S.; Schwalbe, M. Photochemical CO₂ Reduction Catalyzed by Phenanthroline Extended Tetramesityl Porphyrin Complexes Linked with a Rhenium(I) Tricarbonyl Unit. *Inorg. Chem.* **2015**, *54*, 10351–10360.
- (25) Morimoto, T.; Nakajima, T.; Sawa, S.; Nakanishi, R.; Imori, D.; Ishitani, O. CO₂ Capture by a Rhenium(I) Complex with the Aid of Triethanolamine. *J. Am. Chem. Soc.* **2013**, *135*, 16825–16828.
- (26) Mundwiler, S.; Kundig, M.; Ortnr, K.; Alberto, R. A New [2 + 1] Mixed Ligand Concept Based on [^{99m}Tc(OH₂)₃(CO)₃]⁺: a Basic Study. *Dalton Trans.* **2004**, *9*, 1320–1328.
- (27) Gorshkov, N. I.; Schibli, R.; Schubiger, A. P.; Lumpov, A. A.; Miroslavov, A. E.; Suglobov, D. N. “2 + 1” Dithiocarbamate-isocyanide Chelating Systems for Linking M(CO)₃⁺ (M = ^{99m}Tc, Re) Fragment to Biomolecules. *J. Organomet. Chem.* **2004**, *689*, 4757–4763.
- (28) Riondato, M.; Camporese, D.; Martin, D.; Suades, J.; Alvarez-Larena, A.; Mazzi, U. Homo- and Heteroduplex Complexes Containing Terpyridine-Type Ligands and Zn²⁺. *Eur. J. Inorg. Chem.* **2005**, *2005*, 4048–4055.
- (29) Agorastos, N.; Borsig, L.; Renard, A.; Antoni, P.; Viola, G.; Spingler, B.; Kurz, P.; Alberto, R. Cell-Specific and Nuclear Targeting with [M(CO)₃]⁺ (M = ^{99m}Tc, Re)-Based Complexes Conjugated to Acridine Orange and Bombesin. *Chem. - Eur. J.* **2007**, *13*, 3842–3852.
- (30) Gorshkov, N. I.; Lumpov, A. A.; Miroslavov, A. E.; Suglobov, D. N. 2 + 1 Chelating Systems for Binding Organometallic Fragment Tc(CO)₃⁺. *Radiochemistry* **2005**, *47*, 45–49.
- (31) Morais, G. R.; Paulo, A.; Santos, I. Organometallic Complexes for SPECT Imaging and/or Radionuclide Therapy. *Organometallics* **2012**, *31*, 5693–5714.
- (32) Hostachy, S.; Policar, C.; Delsuc, N. Re(I) carbonyl complexes: Multimodal platforms for inorganic chemical biology. *Coord. Chem. Rev.* **2017**, *351*, 172–188.
- (33) Muñoz-Osses, M.; Siegmund, D.; Gómez, A.; Godoy, F.; Fierro, A.; Llanos, L.; Aravena, D.; Metzler-Nolte, N. Influence of the substituent on the phosphine ligand in novel rhenium(I) aldehydes. Synthesis, computational studies and first insights into the antiproliferative activity. *Dalton Trans.* **2018**, *47*, 13861–13869.
- (34) Zobi, F.; Blacque, O.; Jacobs, R. A.; Schaub, M. C.; Bogdanova, A. Y. 17 ϵ rhenium dicarbonyl CO-releasing molecules on a cobalamin scaffold for biological application. *Dalton Trans.* **2012**, *41*, 370–378.
- (35) Lee, L. C.-C.; Leung, K.-K.; Lo, K. K.-W. Recent development of luminescent rhenium(I) tricarbonyl polypyridine complexes as cellular imaging reagents, anticancer drugs, and antibacterial agents. *Dalton Trans.* **2017**, *46*, 16357–16380.
- (36) Chakraborty, I.; Carrington, S. J.; Roseman, G.; Mascharak, P. K. Synthesis, structures, and CO release capacity of a family of water-soluble PhotoCORMs: Assessment of the biocompatibility and their phototoxicity toward human breast cancer cells. *Inorg. Chem.* **2017**, *56*, 1534–1545.
- (37) Leonidova, A.; Gasser, G. Underestimated potential of organometallic rhenium complexes as anticancer agents. *ACS Chem. Biol.* **2014**, *9* (10), 2180–2193.
- (38) Kaplanis, M.; Stamatakis, G.; Papakonstantinou, V. D.; Paravatou-Petsotas, M.; Demopoulos, C. A.; Mitsopoulou, C. A. Re(I) Tricarbonyl Complex of 1,10-Phenanthroline-5,6-dione: DNA Binding, Cytotoxicity, Anti-inflammatory and Anti-coagulant Effects Towards Platelet Activating Factor. *J. Inorg. Biochem.* **2014**, *135*, 1–9.

- (39) Medley, J.; Payne, G.; Banerjee, H. N.; Giri, D.; Winstead, A.; Wachira, J. M.; Krause, J. A.; Shaw, R.; Pramanik, S. K.; Mandal, S. K. DNA-binding and Cytotoxic Efficacy Studies of Organorhenium Pentylcarbonate Compounds. *Mol. Cell. Biochem.* **2015**, *398*, 21–30.
- (40) van Eldik, R.; Summa, N.; Schiessl, W.; Puchta, R.; van Eikema Hommes, N. Thermodynamic and Kinetic Studies on Reactions of Pt(II) Complexes with Biologically Relevant Nucleophiles. *Inorg. Chem.* **2006**, *45*, 2948–2959.
- (41) van Eldik, R.; Soldatovic, T.; Bugarcic, Z. D. Influence of the Chloride Concentration on Ligand Substitution Reactions of [Pt(SMC)Cl₂] with Biologically Relevant Nucleophiles. *Dalton Trans.* **2009**, *23*, 4526–4531.
- (42) Bogojeski, J.; Bugarcic, Z. D.; Puchta, R.; van Eldik, R. Kinetic Studies on the Reactions of Different Bifunctional Platinum(II) Complexes with Selected Nucleophiles. *Eur. J. Inorg. Chem.* **2010**, *2010*, 5439–5445.
- (43) Schutte-Smith, M.; Roodt, A.; Visser, H. G. Ambient and High-pressure Kinetic Investigation of Methanol Substitution in *fac*-[Re(Trop)(CO)₃(MeOH)] by Different Monodentate Nucleophiles. *Dalton Trans.* **2019**, *48*, 9984–9997.
- (44) Schutte, M.; Roodt, A.; Visser, H. G. Coordinated Aqua vs Methanol Substitution Kinetics in *fac*-Re(I) Tricarbonyl Tropolonato Complexes. *Inorg. Chem.* **2012**, *51*, 11996–12006.
- (45) Brink, A.; Visser, H. G.; Roodt, A. Solid State Isostructural Behavior and Quantified Limiting Substitution Kinetics in Schiff-Base Bidentate Ligand Complexes *fac*-[Re(O,N-Bid)(CO)₃(MeOH)]ⁿ. *Inorg. Chem.* **2014**, *53*, 12480–12488.
- (46) Schutte, M.; Kemp, G.; Visser, H. G.; Roodt, A. Tuning the Reactivity in Classic Low-Spin d⁶ Rhenium(I) Tricarbonyl Radiopharmaceutical Synthon by Selective Bidentate Ligand Variation (L,L'-Bid; L,L' = N,N', N,O, and O,O' Donor Atom Sets) in *fac*-[Re(CO)₃(L,L'-Bid)(MeOH)]ⁿ Complexes. *Inorg. Chem.* **2011**, *50*, 12486–12498.
- (47) Malaza, S.; Govender, P.; Schutte-Smith, M.; Visser, H. G.; Smith, G. S. Synthesis and Substitution Kinetics of Tricarbonylrhenium(I) Dendritic Complexes. *Eur. J. Inorg. Chem.* **2017**, *2017*, 3919–3927.
- (48) Brink, A.; Visser, H. G.; Roodt, A. Activation of Rhenium(I) Toward Substitution in *fac*-[Re(N,O'-Bid)(CO)₃(HOCH₃)] by Schiff-Base Bidentate Ligands (N,O'-Bid). *Inorg. Chem.* **2013**, *52*, 8950–8961.
- (49) Manicum, A.; Schutte-Smith, M.; Kemp, G.; Visser, H. G. Illustration of the Electronic Influence of Coordinated β-diketone Type Ligands: A Kinetic and Structural Study. *Polyhedron* **2015**, *85*, 190–195.
- (50) Schutte-Smith, M.; Visser, H. G. The Versatility of Pyridine-2,5-dicarboxylic acid in the Synthesis of *fac*-M(CO)₃ complexes (M = Re, ^{99m}Tc): Reactivity Towards Substitution Reactions and Derivatization After Coordination to a Metal. *Polyhedron* **2015**, *89*, 122–128.
- (51) Salignac, B.; Grundler, P. V.; Cayemittes, S.; Frey, U.; Scopelliti, R.; Merbach, A. E.; Hedinger, R.; Hegetschweiler, K.; Alberto, R.; Prinz, U.; Raabe, G.; Kolle, U.; Hall, S. Reactivity of the Organometallic *fac*-[(CO)₃Re^I(H₂O)₃]⁺ Aquaion. Kinetic and Thermodynamic Properties of HO Substitution. *Inorg. Chem.* **2003**, *42*, 3516–3526.
- (52) Grundler, P. V.; Helm, L.; Alberto, R.; Merbach, A. E. Relevance of the Ligand Exchange Rate and Mechanism of *fac*-[(CO)₃M(H₂O)₃]⁺ (M = Mn, Tc, Re) Complexes for New Radiopharmaceuticals. *Inorg. Chem.* **2006**, *45*, 10378–10390.
- (53) Manicum, A.; Schutte-Smith, M.; Visser, H. G. The Synthesis and Structural Comparison of *fac*-[Re(CO)₃]⁺ Containing Complexes with Altered β-diketone and Phosphine Ligands. *Polyhedron* **2018**, *145*, 80–87.
- (54) Manicum, A.-L. E.; Schutte-Smith, M.; Alexander, O. T.; Twigg, L.; Roodt, A.; Visser, H. G. First Kinetic Data of the CO Substitution in *fac*-[Re(L,L'-Bid)(CO)₃(X)] Complexes (L,L'-Bid = acetylacetonate or tropolonate) by Tertiary Phosphines PTA and PPh₃: Synthesis and Crystal Structures of Water-Soluble Rhenium(I) Tri- and Dicarbonyl Complexes with 1,3,5-Triaza-7-phosphaadamantane (PTA). *Inorg. Chem. Commun.* **2019**, *101*, 93–98.
- (55) Marker, S. C.; MacMillan, S. N.; Zipfel, W. R.; Li, Z.; Ford, P. C.; Wilson, J. J. Photoactivated in Vitro Anticancer Activity of Rhenium(I) Tricarbonyl Complexes Bearing Water-Soluble Phosphines. *Inorg. Chem.* **2018**, *57*, 1311–1331.
- (56) Chen, H.; Parkinson, J. A.; Morris, R. E.; Sadler, P. J. Highly Selective Binding of Organometallic Ruthenium Ethylenediamine Complexes to Nucleic Acids: Novel Recognition Mechanisms. *J. Am. Chem. Soc.* **2003**, *125*, 173–186.
- (57) Bloemink, M. J.; Reedijk, J. Cisplatin and Derived Anti-cancer Drugs, Mechanism and Current Status of DNA Binding. *Met. Ions Biol. Syst.* **1996**, *32*, 641–685.
- (58) Jennerwein, M.; Andrews, P. A. Effect of Intracellular Chloride on the Cellular Pharmacodynamics of *cis*-Diamminedichloroplatinum(II). *Drug Metab. Dispos.* **1995**, *23*, 178–184.
- (59) Kurz, P.; Probst, B.; Spingler, B.; Alberto, R. Ligand Variations in [ReX(Diimine)(CO)₃] Complexes: Effects on Photocatalytic CO₂ Reduction. *Eur. J. Inorg. Chem.* **2006**, *2006*, 2966–2974.
- (60) Smieja, J. M.; Kubiak, C. P. Re(Bipy-tBu)(CO)₃Cl-Improved Catalytic Activity for Reduction of Carbon Dioxide: IR-Spectroelectrochemical and Mechanistic Studies. *Inorg. Chem.* **2010**, *49*, 9283–9289.
- (61) Darensbourg, D. J.; Ortiz, C. G.; Kamplain, J. W. A New Water-Soluble Phosphine Derived from 1,3,5-Triaza-7-Phosphaadamantane (PTA), 3,7-Diacetyl-1,3,7-Triaza-5-Phosphabicyclo[3.3.1]Nonane. Structural, Bonding, and Solubility Properties. *Organometallics* **2004**, *23*, 1747–1754.
- (62) *CrysAlisPRO*; Rigaku: The Woodlands, TX, USA, 2015.
- (63) Sheldrick, G. M. SHELXT – Integrated space-group and crystal-structure determination. *Acta Crystallogr., Sect. A: Found. Adv.* **2015**, *71*, 3–8.
- (64) Sheldrick, G. M. Crystal structure refinement with SHELXL. *Acta Crystallogr., Sect. C: Struct. Chem.* **2015**, *71*, 3–8.
- (65) Müller, P. Practical suggestions for better crystal structures. *Crystallogr. Rev.* **2009**, *15*, 57–83.
- (66) Kurtz, D. A.; Dhakal, B.; Donovan, E. S.; Nichol, G. S.; Felton, G. A. N. Non-photochemical synthesis of Re(diamine)(CO)₂(L)Cl (L = phosphine or phosphite) compounds. *Inorg. Chem. Commun.* **2015**, *59*, 80–83.
- (67) Moore, W. J. *Physical Chemistry*, 4th ed.; Longmans: London, 1962; p 368.
- (68) Salignac, B.; Grundler, P. V.; Cayemittes, S.; Frey, U.; Scopelliti, R.; Merbach, A. E.; Hedinger, R.; Hegetschweiler, K.; Alberto, R.; Prinz, U.; Raabe, G.; Kolle, U.; Hall, S. Reactivity of the Organometallic *fac*-[(CO)₃Re^I(H₂O)₃]⁺ Aquaion. Kinetic and Thermodynamic Properties of H₂O Substitution. *Inorg. Chem.* **2003**, *42*, 3516–3526.
- (69) Barnard, N. I.; Visser, H. G. Novel synthetic method for cobalt complexes: Structural and kinetic study of [Co(NTA)(py)(H₂O)]. *Inorg. Chem. Commun.* **2012**, *15*, 40–42.
- (70) Visser, H. G.; Purcell, W.; Basson, S. S. Kinetic study of the protonations and substitutions of different cobalt(III)-NTA complexes. *Transition Met. Chem.* **2002**, *27*, 461–468.
- (71) Martin, R. B. *Cisplatin: Chemistry and Biochemistry of a Leading Anticancer Drug*; Lippert, B., Ed.; Wiley-VCH: Zurich, Switzerland, 1999; pp 183–205.
- (72) Skiba, J.; Bernás, T.; Trzybński, D.; Wóznia, K.; Ferraro, G.; Marasco, D.; Merlino, A.; Shafikov, M. Z.; Czerwieniec, R.; Kowalski, K. Mitochondria Targeting with Luminescent Rhenium(I) Complexes. *Molecules* **2017**, *22* (5), 809.
- (73) Wang, F.; Chen, H.; Parsons, S.; Oswald, I. D. H.; Davidson, J. E.; Sadler, P. J. Kinetics of aquation and anation of ruthenium(II) arene anticancer complexes, acidity and X-ray structures of aqua adducts. *Chem. - Eur. J.* **2003**, *9*, 5810–5820.